Brain Stimulation 14 (2021) 761–770

Contents lists available at ScienceDirect

Brain Stimulation

journal homepage: http://www.journals.elsevier.com/brain-stimulation

A ventromedial prefrontal dysrhythmia in obsessive-compulsive disorder is attenuated by nucleus accumbens deep brain stimulation

Svenja Treu [a, *], Javier J. Gonzalez-Rosa [a, b], Vanesa Soto-Leon [c], Diego Lozano-Soldevilla [a], Antonio Oliviero [c], Fernando Lopez-Sosa [a, b], Blanca Reneses-Prieto [d], Juan A. Barcia [e], Bryan A. Strange [a]

[a] Laboratory for Clinical Neuroscience, Centre for Biomedical Technology, Universidad Politécnica de Madrid, Spain
[b] University of Cadiz, Institute of Biomedical Research Cadiz (INiBICA), Cádiz, Spain
[c] Hospital Nacional de Parapléjicos, FENNSI Group, Hospital Nacional de Parapléjicos, Toledo, Spain
[d] Department of Psychiatry, Hospital Clínico San Carlos, Instituto de Investigación Sanitaria San Carlos, Universidad Complutense de Madrid, Spain
[e] Department of Neurosurgery, Hospital Clínico San Carlos, Instituto de Investigación Sanitaria San Carlos, Universidad Complutense de Madrid, Spain

ARTICLE INFO

Article history:
Received 16 November 2020
Received in revised form
23 April 2021
Accepted 30 April 2021
Available online 11 May 2021

Keywords:
Obsessive-compulsive disorder
Deep brain stimulation
EEG
Nucleus accumbens
Ventromedial frontal cross-frequency coupling

ABSTRACT

Background: Obsessive-compulsive disorder (OCD) has consistently been linked to abnormal frontostriatal activity. The electrophysiological disruption in this circuit, however, remains to be characterized.
Objective/hypothesis: The primary goal of this study was to investigate the neuronal synchronization in OCD patients. We predicted aberrant oscillatory activity in frontal regions compared to healthy control subjects, which would be alleviated by deep brain stimulation (DBS) of the nucleus accumbens (NAc).
Methods: We compared scalp EEG recordings from nine patients with OCD treated with NAc-DBS with recordings from healthy controls, matched for age and gender. Within the patient group, EEG activity was compared with DBS turned off *vs.* stimulation at typical clinical settings (3.5 V, frequency of stimulation 130 Hz, pulse width 60 μs). In addition, intracranial EEG was recorded directly from depth macroelectrodes in the NAc in four OCD patients.
Results: Cross-frequency coupling between the phase of alpha/low beta oscillations and amplitude of high gamma was significantly increased over midline frontal and parietal electrodes in patients when stimulation was turned off, compared to controls. Critically, in patients, beta (16–25 Hz) -gamma (110–166 Hz) phase amplitude coupling source localized to the ventromedial prefrontal cortex, and was reduced when NAc-DBS was active. In contrast, intracranial EEG recordings showed no beta-gamma phase amplitude coupling. The contribution of non-sinusoidal beta waveforms to this coupling are reported.
Conclusion: We reveal an increased beta-gamma phase amplitude coupling in fronto-central scalp sensors in patients suffering from OCD, compared to healthy controls, which may derive from ventromedial prefrontal regions implicated in OCD and is normalized by DBS of the nucleus accumbens. This aberrant cross-frequency coupling could represent a biomarker of OCD, as well as a target for novel therapeutic approaches.

Introduction

Obsessive-compulsive disorder (OCD) is a neuropsychiatric disease characterized by recurrent intrusive thoughts (obsessions) and/or uncontrollable repetitive actions (compulsions) [1], with a lifetime prevalence of 2.3% [2]. The pathology of OCD has been linked to abnormal structure and function within a frontostriatal network including nucleus accumbens (NAc) and medial frontal cortex [3–8]. Deep brain stimulation (DBS) targeting the NAc is

Abbreviations: DBS, deep brain stimulation; iEEG, intracranial EEG; NAc, nucleus accumbens; OCD, obsessive-compulsive disorder; PAC, phase amplitude cross-frequency coupling; PD, Parkinson's disease; STN, subthalamic nucleus; VC/VS, ventral capsule/ventral striatum; YBOCS, Yale-Brown Obsessive-Compulsive Scale.

* Corresponding author. Laboratory for Clinical Neuroscience, Universidad Politécnica de Madrid, Centro de Tecnología Biomédica, Parque Científico y Tecnológico de la U.P.M. Campus de Montegancedo. Ctra. M 40-Km.38, 28223 Pozuelo de Alarcón. Madrid, Spain.;
E-mail address: svenja.treu@ctb.upm.es (S. Treu).

https://doi.org/10.1016/j.brs.2021.04.028

increasingly used in the treatment of medication-resistant OCD. In these patients, NAc-DBS normalizes excessive frontostriatal connectivity measured with resting state functional MRI, with this connectivity reduction shown to correlate with improvement in obsessions and compulsions [9]. Scalp EEG recordings show that DBS attenuates delta amplitude (1–4 Hz) [9], but slow oscillations are similar across off/on states in treatment responders at rest [8,10]. Indeed, the majority of studies investigating electrophysiological markers of psychiatric disease focus on alterations of oscillatory power in different frequency bands.

Recently, however, a range of neurological and psychiatric diseases, including schizophrenia, Parkinson's disease (PD), autism, and Alzheimer's disease have been linked to pathological synchronization of neuronal activity [11,12]. An initial observation of increased beta-high gamma phase amplitude cross-frequency coupling (PAC) in primary motor cortex was made in PD, and shown to be reduced by DBS of the subthalamic nucleus (STN) [13]. Essential tremor, on the other hand, is associated with increased alpha-high gamma PAC in the sensorimotor cortex [14]. With respect to psychiatric conditions, one study in seven OCD patients treated with NAc-DBS reported that PAC between the phase of beta/low gamma frequencies and the amplitude of broadband gamma frequencies was suppressed by DBS [15]. However, this study selectively focused on scalp EEG responses at one mid-occipital electrode, despite the extant evidence implicating frontostriatal circuit dysfunction in OCD. Whether the observed occipital PAC is related with the pathology of OCD cannot be concluded from this study, since no data from healthy control subjects was recorded. Moreover, applying the same analysis to scalp EEG resting state recordings from five patients treated with DBS for major depressive disorder failed to replicate the finding of suppressed occipital PAC induced by NAc-DBS [16].

We set out to resolve these discrepant findings by examining scalp EEG resting state data recorded in 10 OCD patients implanted for NAc-DBS. In view of evidence for excessive frontostriatal connectivity in OCD and its alleviation by NAc-DBS, we predicted aberrant PAC in patients compared to healthy control subjects in frontal regions, which would be modulated under active NAc-DBS. Critically, we adopted a whole-brain approach, without restricting our analyses to a specific neuroanatomical region or frequencies of interest. Lastly, we tested whether this aberrant PAC is also observed in direct intracranial EEG recordings from the NAc in four patients.

Methods and materials

Participants

Ten patients with treatment-resistant OCD and nine control subjects participated in this study after giving written consent according to the Declaration of Helsinki. One patient was excluded due to poor EEG data quality. The remaining nine patients (three female) were aged 20–52 years (mean: 35). Further patient details are provided in Table 1. All patients had been implanted with bilateral DBS electrodes in the NAc 1–60 months before the study (mean: 35). In all patients except for one, Medtronic (Fridley, MN, USA) Model 3391 stimulating macroelectrodes were inserted, with the most distal contacts within the posterior part of the NAc. In patient 9, the most distal contacts were slightly dorsal to target and in patient 10, Boston Scientific (Marlborough, MA, USA) DB-2201 electrodes were used. A summary of group electrode locations, produced with Lead-DBS software [17] is provided in Fig. 1. A control group of nine neurologically and psychiatrically healthy volunteers was selected, matched in terms of age and sex. In addition, intracranial resting state recordings from the NAc were recorded in four patients (two female, age range: 30–40, mean: 36), two of them being part of the scalp EEG cohort. The study was approved by the ethics committee of the Hospital Clinico San Carlos, Madrid, Spain (study code PI10/1932 10/131).

Scalp EEG resting state recordings

Prior to EEG recording, stimulators were turned off for a "washout" period of 2 h. In five patients, a 64-channel EEG cap was used, in the remaining subjects EEG activity was recorded with a 96-channel cap, following the 10/20 EEG International System and with a sampling frequency of 500 Hz, using average reference. Spontaneous EEG activity at rest was recorded during the two conditions "eyes open off" and "eyes open DBS on" for 3 min, respectively. Bilateral stimulation was bipolar, between the two most distal contacts and delivered at 3.5 V and 130 Hz (pulse width 60 μs). Patients were blind about the onset of the transient stimulation.

Scalp EEG data analysis

Preprocessing of the data was performed using *Brainstorm version 3.4* (http://neuroimage.usc.edu/brainstorm) [18]. Baseline correction was applied, as well as a high-pass filter of 0.5 Hz, a Butterworth Bandstop filter (+- 3 Hz) for 50 Hz and 100 Hz line noise and for the stimulation frequency of 130 Hz. Signals were inspected visually to remove large artifacts whereas for smaller artifacts, like eye blinks and movements, an independent component analysis procedure with the JADE algorithm [19] was used. Noisy and flat channels were discarded.

For the analysis of power differences, power spectral densities (PSD) were calculated using the Welch method (overlap of 50%, windows of 4 s) and divided by total power for spectrum normalization. A Monte-Carlo cluster-permutation test was then conducted, comparing controls *vs.* patients, and subsequently off *vs.* on DBS in the patient group, performing two-tailed t-tests with a cluster-level alpha of 0.05 and 1000 randomizations.

Phase amplitude coupling was calculated with phase frequencies from 2 to 30 Hz and amplitude frequencies from 40 to 166 Hz, based on the approach implemented in *Brainstorm* [20]. These coupling values were exported to *Matlab* (The MathWorks, Inc., Natick, Massachusetts, USA) and the *FieldTrip* toolbox (Nijmegen, The Netherlands; [21]) was employed to conduct a Monte-Carlo cluster-permutation test with the two cluster-levels *phase frequency* and *amplitude frequency*. The Monte-Carlo method corrects for multiple comparisons on these levels [22]. For the comparison of PAC between the healthy control group and patients off stimulation, electrodes were then grouped into 10 distinct scalp portions illustrated in supplementary Fig. S1. PAC values were averaged within each scalp grouping and independent two-sided t-tests performed, testing the independent variable patient *vs.* control, with a cluster-level alpha of 0.01 and 1000 randomizations, and the ensuing p-value Bonferroni corrected for the comparison of 10 scalp electrode groups.

Next, to test the hypothesis of reduced PAC during NAc-DBS on *vs.* off conditions, patient EEG recordings were analyzed in source space for improved localization of brain areas contributing to the signal recorded on scalp level. Patients' pre-operative MRI T1 images were used to create a realistic head model. Pial surfaces were extracted within *BrainSuite17a* (UCLA Brain Mapping Center, San Francisco, USA; [23]) and read into *Brainstorm*. The cortical surface was down-sampled to 3000 vertices and for each subject a forward head model was computed using a 3-shell sphere. Signals were source localized by applying a minimum-norm imaging technique, with constrained dipole orientations, and finally projected to an

Table 1
Patients' details. * indicate patients with intracranial NAc recordings. NA not applicable. Medication pertains to the time of recording electrophysiological data. ˢpertains to the time of surgery for the two patients who did both scalp and iEEG recordings. † At disease onset, this patient presented with cleaning, checking and order compulsions, which responded to pharmacotherapy. His score on the Yale–Brown Obsessive Compulsive Scale is in the mild range, which reflects the relative insensitivity of this scale to primarily obsessive symptomatology.

Patient	Gender	Age at surgery	Months of chronic stimulation	Pre-operative YBOCS	% YBOCS change (Ø contact 0&1)	Medication (in mg)
1	f	49	41	36	0.41	Lorazepam 7.5, Valproic Acid 1000, Venlafaxine 225
2	f	37	60	32	0.32	Clomipramine 225, Sertraline 75, Eutirox 100
3	f	28	47	29	0.25	Sertralina 75
4	m	28	35	13†	0.2	Clomipramine 150, Sertraline 200
5	m	21	47	24	0.14	Escitalopram 20, Clomipramine 25, Clonazepam 0,5
6	m	50	5	38	0.23	Clomipramina 175, Sertraline 100, Diazepam 5, Enalapril 10
7*	m	39	24	37	0.33	Olanzapine 5, Fluvoxamine 300, Clonazepam 3 *(4ˢ)*
8*	m	36	6	36		Venlafaxine 150 *(225ˢ)*, Quetiapine 300 *(150ˢ)*, Aripiprazol 30 *(0ˢ)*, Ketazolam 30 *(0ˢ)*, Clonazepam 6 *(0ˢ)*
9	m	20	1	40	0.24	Clomipramine 150, Sertraline 200, Olanzapine 20, Lorazepam 4, Reboxetine 4
10*	f	40	NA	31		Sertraline 100, Pregabalin 300, Venlafaxine 150, Clorazepate dipotassium 30
11*	f	30	NA	30	0.16	Clomipramine 150, Citalopram 40, Pregabalin 45, Lormetazepam 2

MNI (ICBM152) template. This was then clustered into 50 equally sized "patches" of cortical surface. For the projected signal corresponding to each patch, PAC was calculated and exported to Fieldtrip. Two-tailed, paired t-tests were performed for each of the 50 patches, testing the independent variable stimulation off *vs.* on, with a cluster-alpha of 0.01 and 1000 randomizations. Given that this analysis entails testing of 50 cortical patches, the false discovery rate (FDR) method was chosen for a less conservative correction for multiple comparisons, in contrast to Bonferroni correction for the scalp cluster comparison.

NAc intracranial EEG resting state recordings

Intracranial EEG (iEEG) activity was acquired from macroelectrodes during the 4th-5th post-operative day, with externalized leads, prior to generator implantation. Data were acquired using Spike2 software (Cambridge Electronic Design, Cambridge, UK), at a sampling rate of 5000-Hz, amplified with a factor of 30000 and bandpass filtered between 0.5 and 1.000 Hz. A bipolar montage was used in two patients, whereas in the other two patients monopolar recordings of the eight channels were referenced to the right mastoid.

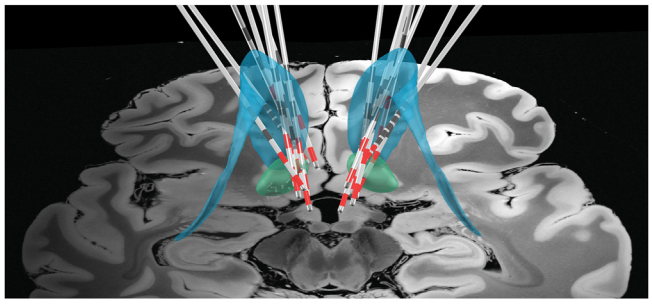

Fig. 1. *Group DBS electrode localization*. Bilateral electrode implantation of all 9 patients, reconstructed using *Lead DBS*. Contacts stimulated during the EEG recording are highlighted in red. NAc (green) and caudate (blue) are derived from the CIT168 Reinforcement Learning Atlas (https://neurovault.org/collections/3145/). The background template is a 100-μm T1 scan of an ex-vivo human brain, acquired on a 7 T MRI scanner (https://openneuro.org/datasets/ds002179/versions/1.1.0). (For interpretation of the references to color in this figure legend, the reader is referred to the Web version of this article.)

NAc intracranial EEG data analysis

In all four patients, a bipolar montage between the two most ventral, NAc contacts was applied. Due to artefactual noise, the right most ventral contact in two patients had to be rejected, so that only the left side of these patients was included in the analysis, which was also carried out using *Brainstorm*. Preprocessing included downsampling to 500Hz, detrending, the application of a high-pass filter of 0.5 Hz and a Butterworth Bandstop filter (+- 3 Hz) for 50 Hz and 100 Hz line noise. Artifacts were rejected by visual inspection and PAC and PSD were calculated in the same way as for scalp EEG. Statistics were not performed on these data, due to the low number of observations.

Beta waveform analysis

Recent studies have revealed that the waveform of neuronal oscillations frequently deviates from a sinusoidal form [24] and that artefactual, spurious coupling can be produced by sharp edges in time series data [25]. To address the possibility that non-sinusoidality of beta oscillations contributed to our measures of PAC, and their modulation under DBS, we characterized the wave morphology of beta oscillations using the sharpness and steepness indices proposed in Cole et al. [26]. The two measures have been successfully applied to human beta oscillations in patients suffering Parkinson using intracranial and scalp recordings [26,27]. In brief, the sharpness index measures the wave asymmetry relative to the x-axis. To calculate this index, we first bandpass filtered the raw voltages of the electrodes of interest within the beta band (14–35Hz). Peaks and troughs were found in the raw time series as the positive and negative extrema situated between the zero-crossing points. Peak and trough sharpness were defined as the voltage difference between 5 data points before and after the peak/trough respectively. Finally, Sharpness ratio was defined as the log of the maximum ratio of either mean peak sharpness to mean trough sharpness, or vice versa [26]. In a complementary manner, the steepness ratio measures the wave asymmetry relative to the y-axis. Rise and decay steepness were defined as the maximum of the first temporal derivative between the trough and the peak, or the peak and the trough, respectively [26]. The steepness ratio was defined in an analogous way as the sharpness ratio but using rise and decay steepness.

To test whether beta sharpness and/or steepness ratio correlate with PAC magnitude, we employed the same PAC index defined in

Özkurt et al. 2011 [28], as this is the method used by Cole et al. Although this PAC calculation differs slightly from the method implemented in *Brainstorm*, we note that Cole et al. [26] showed their results to be similar when applying alternative metrics of statistical PAC, including that of Canolty et al. [20]. We then calculated Spearman rho correlation between PAC magnitude and beta sharpness and/or steepness ratio, and compared these correlations on *vs*. off DBS.

Finally, peak triggered averages were performed following Cole et al. [26] (see supplementary Fig. S2B). Peaks previously identified during the computation of the sharpness index were used as events to average a ±0.2 s window. Note that we restricted our analysis to only the top 10% of gamma amplitude.

Results

Scalp EEG

We first tested for group-dependent differences in scalp-recorded phase amplitude coupling between the OCD patients off DBS *vs*. the matched control group. As predicted, patients showed higher PAC than controls, with significant clusters ranging between phase frequencies of 2–23 Hz (most pronounced around 10 Hz) and amplitude frequencies of 102–166 Hz (Fig. 2A and B). These differences were observed over midline frontal (summed t-values = 664; $p_{corr}<0.025$) and centroparietal (summed t-values = 836; $p_{corr}<0.025$) electrodes (highlighted in Fig. 2C). A separate *t*-test including only electrode Oz, in an attempt to replicate previous findings [15], did not reach significance. To test for possible power differences between patients and controls, a cluster-permutation testing was applied. Significantly increased beta power in patients was found between 18 and 36 Hz (summed t-values = 205.46; $p < 0.025$; Fig. 3A).

We next tested whether NAc stimulation would modulate the elevated PAC observed in the patient group. To facilitate inference regarding spatial localization of these effects, scalp recorded potentials were inverted to cortical source space for this analysis. Based on the difference between patients off *vs*. the control group, phase frequencies from 2 to 25 Hz and amplitude frequencies from 100 to 166 Hz were selected for the Monte-Carlo cluster-permutation test on phase amplitude coupling, including all 50 cortical surface patches. NAc-DBS on *vs*. off resulted in a significant

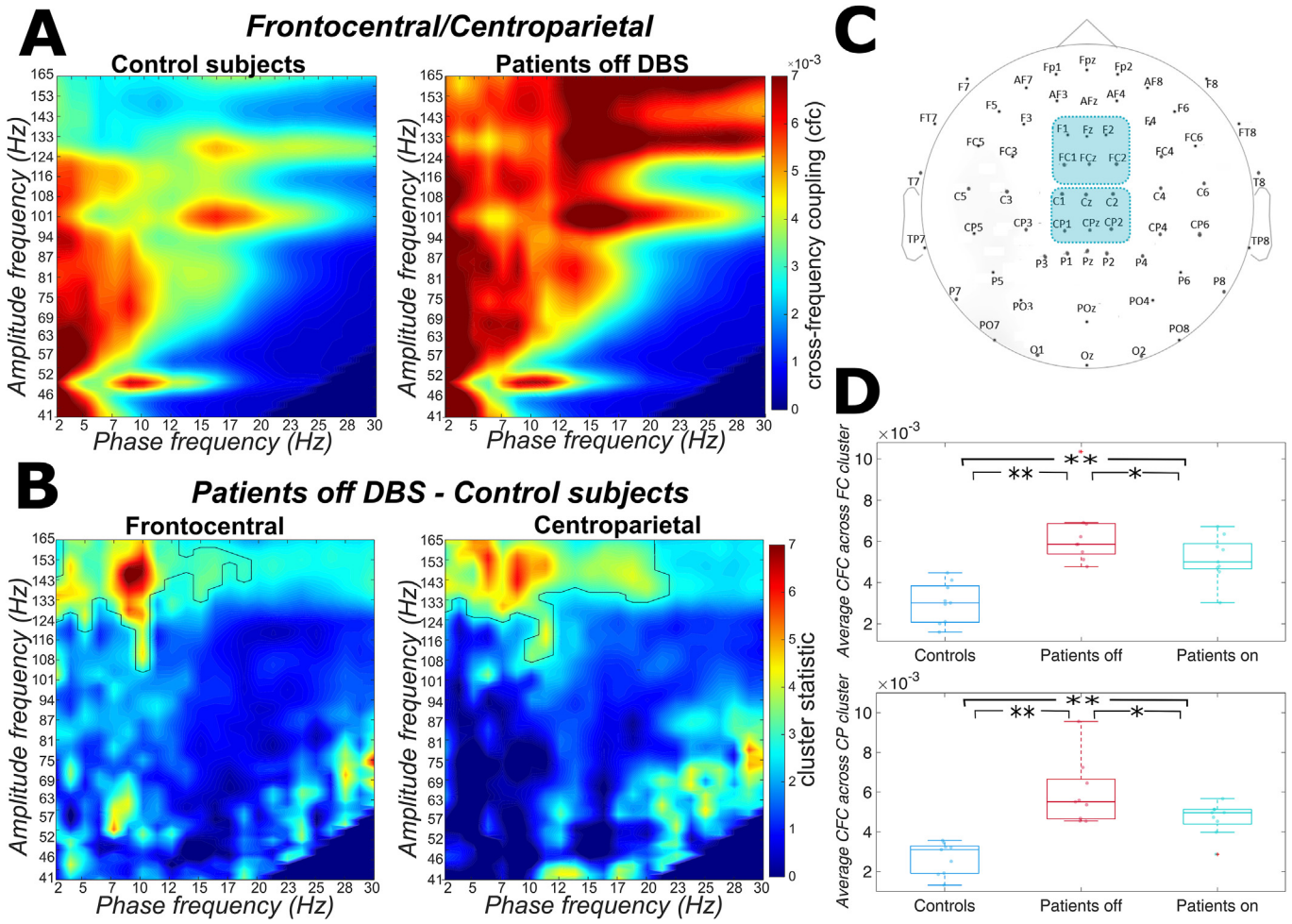

Fig. 2. *Cross-frequency coupling is greater in OCD patients than controls and reduced by NAc-DBS in OCD patients.* A) Average across the midline frontal sensors with significantly stronger PAC in patients off DBS *vs*. control subjects. B) Cluster statistic resulting from the *t*-test comparing patients off *vs*. control subjects. Black contours represent the significant clusters, covering a range of phase frequencies of up to 23 Hz and amplitude frequencies between 102 Hz and 166 Hz. C) Schematic of the two significant frontocentral and centroparietal sensor groups. D) Average PAC across the two clusters for control subjects *vs*. patients (shown here for both off and on DBS). Frontocentral PAC is significantly lower in control subjects than patients off DBS ($t(16) = 5.25$) and patients on DBS ($t(16) = 4.36$), and is significantly reduced by DBS in patients ($t(8) = 2.47$). Centroparietal PAC is significantly lower in control subjects than patients off DBS ($t(16) = 5.37$) and patients on DBS ($t(16) = 5.15$), and is significantly reduced by DBS in patients ($t(8) = 2.57$). *paired t-tests: $p_{uncorr.}<0.05$; **independent t-tests: $p_{uncorr}<0.001$.

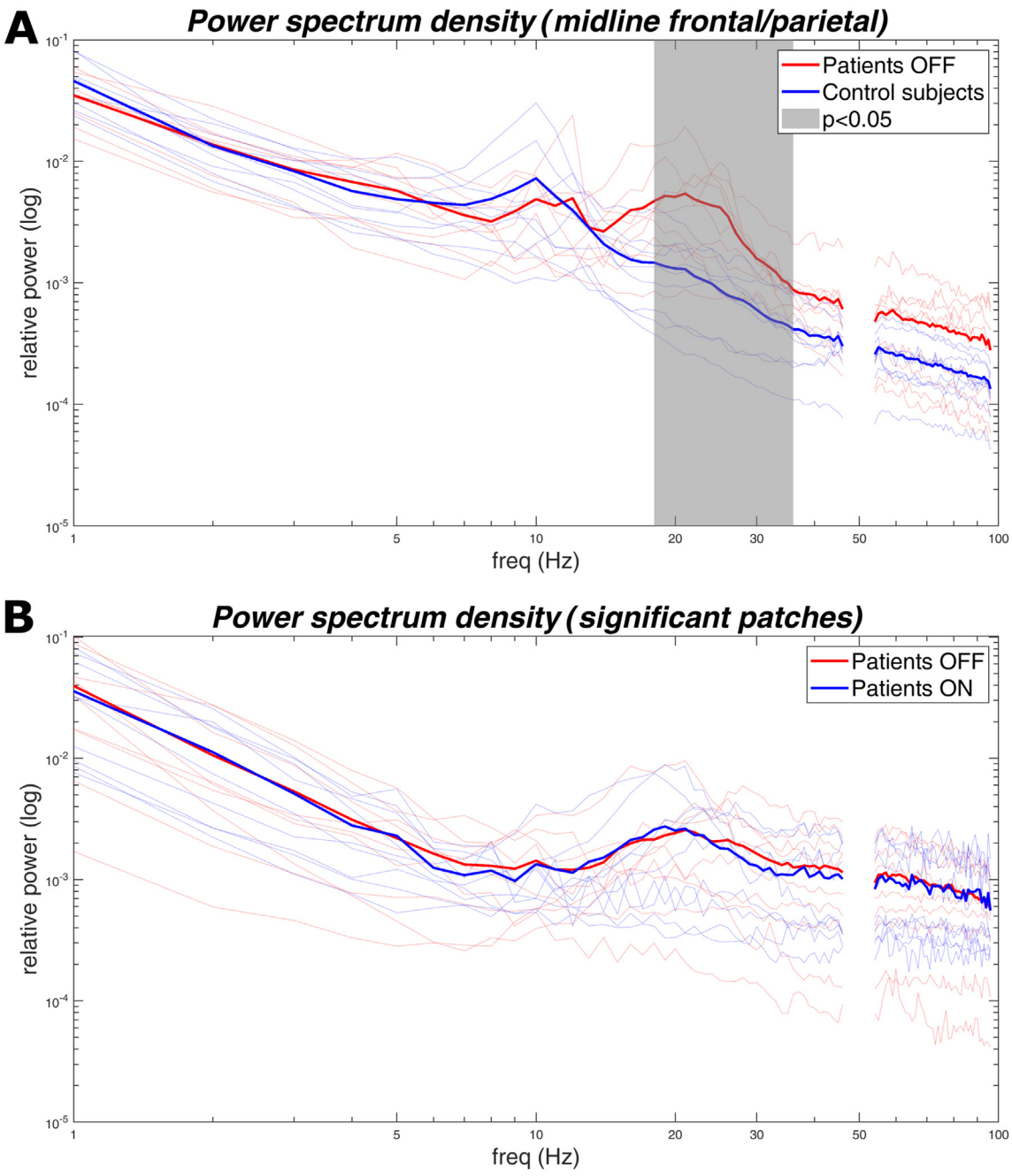

Fig. 3. *Power spectrum densities*. Power spectral densities (PSD) were calculated using the Welch method (overlap of 50%, windows of 4 s) and divided by total power for spectrum normalization. Monte-Carlo cluster-permutation tests were applied to compare the power spectra between controls and patients (A) as well as between off *vs.* on DBS (B). While beta power was significantly increased in patients *vs.* controls (summed t-values = 205.46; $p < 0.025$), with the significant frequency cluster highlighted in gray, no power differences were observed between off *vs.* on conditions in patients at the source level, averaged across both significant patches. Spectral discontinuities are due to bandstop filtering of line noise.

reduction of PAC in two patches in ventromedial prefrontal cortex, extending into orbitofrontal areas (Fig. 4A and B), after FDR correction. The two clusters (summed t-values = 398.629; $p_{corr} = 0.05$; summed t-values = 347.882; $p_{corr} = 0.05$) spanned frequencies between beta (16–25 Hz) and high gamma (110–166 Hz), with the most pronounced reduction of PAC between phase frequencies of 20–24 Hz and amplitude frequencies of 133–143 Hz (Fig. 4C). This observed effect cannot be explained by NAc-DBS effects on oscillatory power, as the PSDs do not differ across the two conditions (Fig. 3B).

To further elucidate whether DBS led to a normalization of abnormal frontal PAC in patients, we calculated the average of PAC across the two significant clusters on scalp level for the three conditions *controls*, *DBS off* and *DBS on*. Pairwise comparisons (two between-group independent t-tests and one paired *t*-test for the within-patient comparison off *vs.* on) showed, that despite frontocentral and centroparietal PAC being significantly reduced by NAc-DBS, patient beta-gamma PAC during NAc-DBS still remained significantly higher than in control subjects (Fig. 2D).

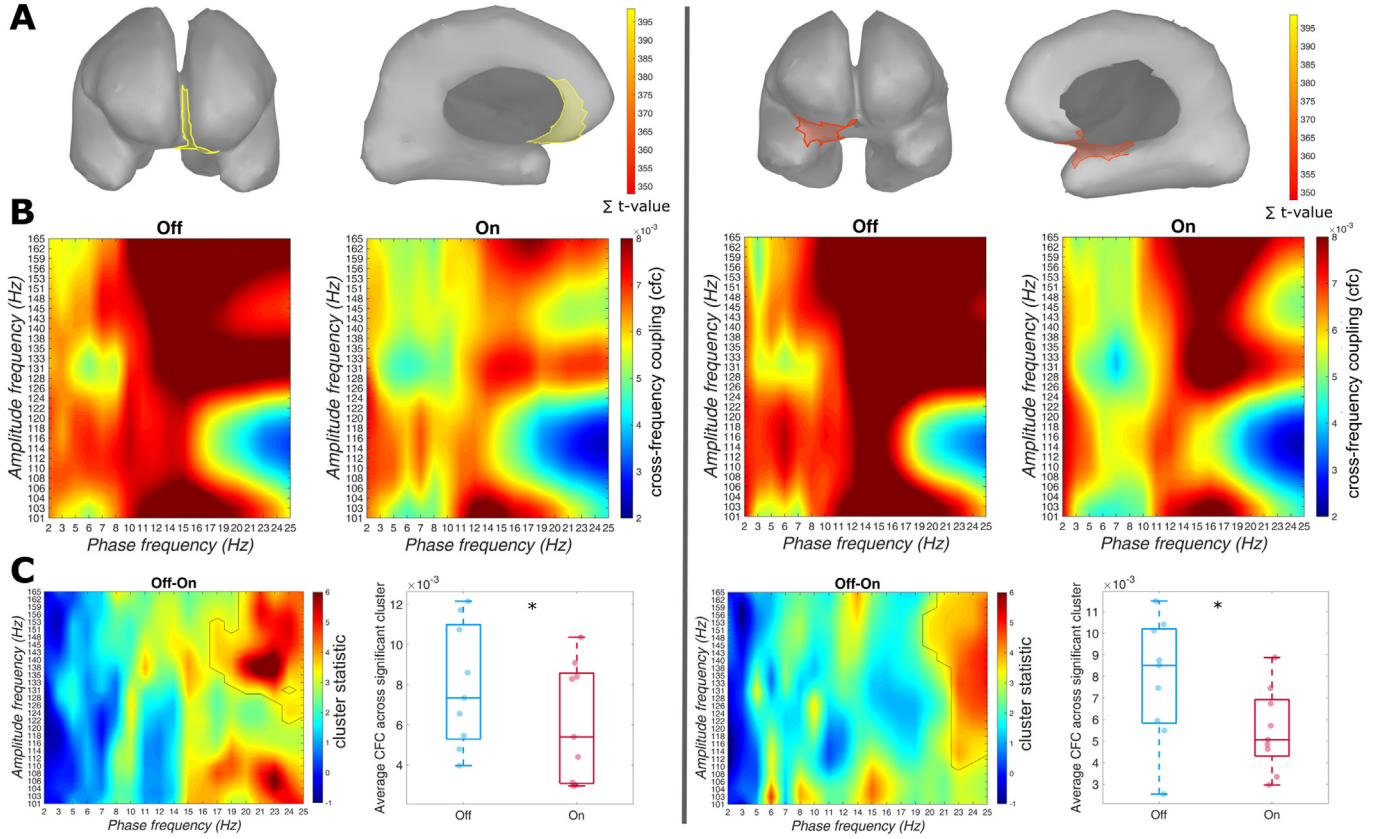

Fig. 4. *Ventromedial-orbitofrontal cross-frequency coupling is significantly reduced by NAc-DBS.* A) Significant patches in ventromedial prefrontal cortex (left panels), extending into orbitofrontal cortex (right panels), colored by their cluster t-value and superimposed on an MNI (ICBM152) brain template. B) Average co-modulogram of NAc-DBS off *vs.* on for the two significant source patches, respectively. C) Cluster statistics resulting from the *t*-test comparing NAc-DBS off *vs.* ons, with black contours highlighting the significant clusters, encompassing beta phase frequencies from 16 to 25 Hz and high gamma amplitude frequencies (110–166 Hz). Boxplots represent the average and individual patient (○) PAC across the significant clusters, respectively, for the two DBS states off *vs.* on. * $p_{corr} = .05$.

Lastly, we tested for a correlation between the reduction of the patients' OCD symptoms and reduction of PAC comparing on *vs.* off across patients. As reported previously [29], patients were evaluated with the Yale-Brown Obsessive-Compulsive Scale (YBOCS) prior to surgery and then after three months of bilateral stimulation of each of the four electrode contacts. For one of the patients, clinical improvement after stimulation of contact 1 was not assessed. Thus, for each of the remaining eight patients, PAC reduction was averaged across the two significant surface patches and correlated with average symptom reduction following monopolar stimulation of the two NAc contacts following three months stimulation. We did not find a significant correlation (Kendall's tau = 0; p = 1).

Beta waveform

Previously, it has been reported in PD patients undergoing DBS to the subthalamic nucleus that non-sinusoidal, asymmetric waveform features of beta, *i.e.*, the sharpness ratio between peaks and troughs, correlate with beta-high gamma phase-amplitude coupling in the motor cortex and are diminished by DBS [26]. This non-sinusoidal nature of oscillations raises special challenges in data analysis, but it also provides new and unique insight regarding the underlying physiology of these rhythms [24,30]. To test whether the non-sinusoidality of beta may contribute to the aberrant PAC we observe in OCD patients off stimulation, we calculated these waveform features following the same approach as applied to PD [26]. We did find a significant correlation between beta-gamma cross-frequency coupling (CFC) (14–35Hz/60-166Hz) and the sharpness and steepness ratio of beta for the DBS off state, but, critically, this is not modulated by DBS. Wilcoxon signed rank tests show no significant changes of sharpness ($Mdn_{off} = 0.0296$; $Mdn_{on} = 0.0174$; T = 31; z = −1; p = 0.3) or steepness ($Mdn_{off} = 0.0204$; $Mdn_{on} = 0.0171$; T = 27; z = −0.53; p = 0.6) ratios induced by DBS. This implies that DBS leads to reduced pathological phase-amplitude CFC, rather than to a smoothing of the beta waveform (see supplementary Fig. S2).

NAc intracranial EEG

PAC measures were averaged across the six bipolar recordings (two bilateral and two on the left side). Localizations of the macroelectrodes and all contacts included in the analysis are presented in Fig. 5A. By contrast to the scalp EEG results, no PAC between the phase of beta and high gamma amplitude was observed in the NAc, where a stronger coupling is present between the phase of delta-theta and broadband gamma amplitude (Fig. 5B). Thus, the increased beta-gamma coupling observed on the scalp level cannot be explained by a conduction effect from the nucleus accumbens. The power distribution measured in the NAc is similar to that on the scalp level, with pronounced beta activity (Fig. 5C).

Discussion

We demonstrate that PAC between alpha/beta and gamma in OCD patients is significantly increased in fronto-central scalp

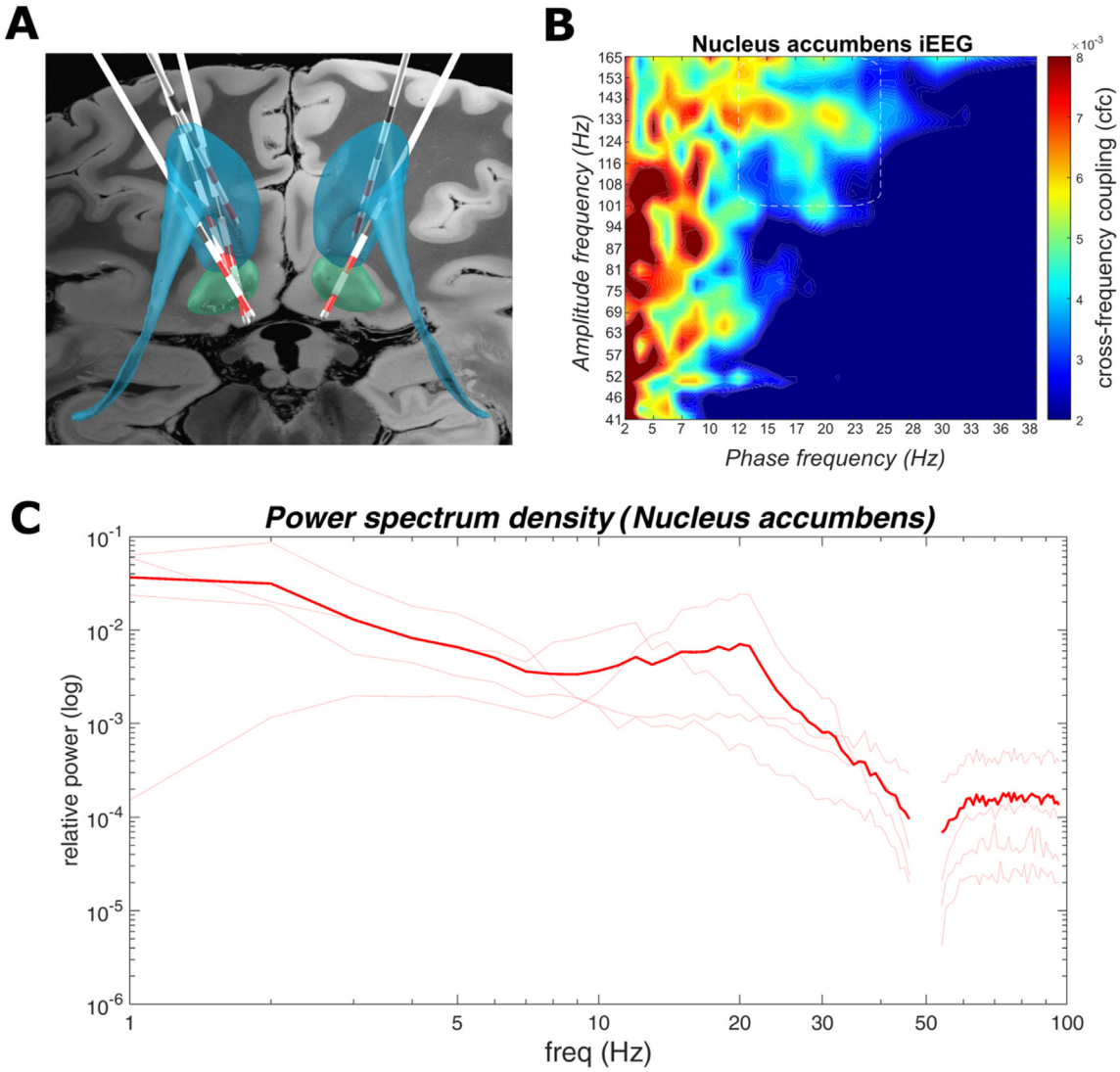

Fig. 5. *Intracranial EEG recorded in the nucleus accumbens.* A) Localization of iEEG electrodes. Bipolar recordings were analyzed from contacts highlighted in red. Lead DBS software was used for reconstruction and same background template and atlas as in Fig. 1. B) Within the nucleus accumbens, no phase amplitude coupling was observed between high alpha/beta and high gamma, as indicated by the white dashed rectangle. Coupling seems to be stronger between the phase of delta-theta and broadband gamma. C) The power distribution measured in the NAC is similar to the scalp EEG, with a pronounced beta activity. (For interpretation of the references to color in this figure legend, the reader is referred to the Web version of this article.)

sensors, which seem to arise from ventromedial prefrontal sources implicated in the pathophysiology of OCD. This result advances previous findings [15,16] by adopting a whole brain approach to detect anatomically-specific effects in ventromedial prefrontal cortex, and by directly comparing neural oscillations in patients with a matched healthy control group. By doing so, we support suggestions that OCD pathophysiology may involve abnormal oscillatory coupling. Moreover, we show that deep brain stimulation of the NAc attenuates this abnormality. Intracranial recordings from the NAc in four patients, did not reveal the same pattern of coupling between beta phase and gamma amplitude, indicating that aberrant PAC observed in scalp recordings is unlikely attributable to conduction from the NAc. Even though we observed significantly increased beta power in patients, we cannot be certain whether this reflects disease pathology or medication (pharmacological regimes for all patients is given in Table 1).

In PD patients, subthalamic DBS was shown to alleviate excessive beta-gamma coupling in the motor cortex [13]. Moreover, the level of cortical PAC correlated with disease severity and subthalamic DBS-induced PAC reductions were associated with motor symptom improvements. By contrast, we did not observe a correlation between PAC reduction and OCD symptom reduction after 3 months of NAc-DBS in our patients. Although subtle differences in stimulation parameters between the EEG session and the clinical evaluation [29] exist, we interpret these results in terms of a patient-specific effect. That is, reduction of anomalous medial frontal and orbitofrontal PAC evoked by NAc-DBS may contribute to symptom reduction in all patients, but reduction in YBOCS also reflects an additional effect of DBS on certain other frontostriatal circuits that are specific to each patient [29]. Thus, even though across patients, the strongest reduction of PAC was found in the ventromedial regions reported here, depending on the patients' individual symptomatology, excessive PAC in differing frontal subregions may also underlie their respective obsessions/compulsions. This is supported by the observation that the biggest PAC differences between off and on NAc-DBS are found in different frontal patches across subjects (see supplementary Fig. S3). In support of a key role of medial frontal modulation in the clinical

benefit of NAc-DBS, including the effects of DBS of all four electrode contacts in the current cohort and using a normative structural connectome, we recently reported a positive association between clinical improvement and structural connectivity to ventromedial prefrontal areas [31]. Furthermore, tractography studies in patients from the current cohort show that the primary cortical target of the stimulated NAc site is the ventromedial PFC [32].

Our results raise a possibility that abnormally elevated PAC may be a generic pathological feature in different neurological and psychiatric diseases in which basal ganglia are involved (e.g. PD and, as described here, OCD). It is relevant in this regard that alpha-gamma PAC has been observed in the NAc of patients with treatment-refractory major depression [33]. In PD, accordingly, elevated beta-high gamma coupling in the STN has been reported [34]. Notably, in another study on PD patients, elevated low beta-gamma coupling was higher in the more affected hemisphere [35], which supports the idea of a pathologically increased PAC within subcortical structures related to the disease, in addition to cortical areas, where electrophysiological recordings from healthy subjects are available. To date, the phenomenon of beta-gamma coupling has only been studied in detail in PD and the exact physiological meaning remains uncertain. In general, beta-gamma coupled oscillations have been considered an important mechanism for integrating different reward and learning processes, which are known to be maladaptive in OCD [36,37] and which involve an extended network, including the ventromedial prefrontal cortex and the ventral striatum [38–40]. Cross-frequency coupling is thought to be the underlying process for the communication between local and distant brain structures, with local processing reflected by high-frequency oscillations and distant brain activity synchronized by low-frequency oscillations [41]. In PD, the observed excessive PAC in the motor cortex was suggested to hinder the flexible onset of movements [42], which was shown to rely on a reduction of PAC [43,44]. It is conceivable, that the observed frontal PAC in OCD similarly disables dynamic neuronal input from other cortical regions, leading to the rigid and repetitive behavior, typical for this disease. Consequently, the reduction of this dysrhythmia could be one mechanism of action of NAc-DBS in the clinical improvement in these patients. The role of abnormal beta-gamma rhythms within the frontostriatal network in OCD is further supported by a recent study demonstrating that obsessive-compulsive behavior was attenuated by applying alternating current over the orbitofrontal cortex in a non-clinical sample.

The fact that excessive beta-gamma coupling is a shared feature between OCD and PD raises the question of whether there is a potential overlap in pathophysiology between the two diseases [45]. A recent meta-analysis identified OCD as a possible risk factor for subsequently developing PD [46]. While most studies of PAC in PD patients have exclusively focused on motor cortex oscillations, a recent scalp EEG study with whole-brain source localization demonstrated beta-gamma coupling in dorsolateral prefrontal, premotor cortex, primary motor and somatosensory cortices, greater in the hemisphere contralateral to the clinically more affected side [47]. Aberrant mediofrontal synchronization was not observed in PD [47], pointing to a potential neuroanatomical difference between OCD and PD for a shared underlying neurophysiological abnormality.

By contrast to observations from subcortical structures in PD and depression patients, we do not observe abnormal PAC in the NAc itself in any of the four OCD patients tested. This could point to a primarily cortical pathology underlying aberrant PAC in OCD. Relevant to this proposal is the recent suggestion that scalp EEG recorded PAC in PD could be a manifestation of the activity of two physiologically distinct oscillators from two spatially distinct cortical substrates [47]. The interpretation of our intracranial analysis is, however, clearly limited by the small sample size and further recordings are required to systematically compare the cortical pattern of PAC to oscillations within the accumbens. We acknowledge as a further limitation that direct NAc recordings were performed in the immediate post-operative period, whereas scalp EEG recordings were acquired up to several years post-implantation. In future studies, simultaneous recordings from electrodes in the NAc and scalp electrodes will inform not only about local, but also about interregional effects of DBS on PAC [8].

One important, and often overlooked, confound of PAC is the non-sinusoidal waveform morphology of the phase frequency, which can produce spurious high-frequency components unrelated to veridical PAC. This motivated an analysis of beta waveforms, which indeed demonstrated that beta-gamma PAC correlates strongly with the sharpness index of the beta waveform as described previously in PD recordings [26] (Fig. S2A). An additional phase-locked plot of the averaged gamma peaks further indicates that at least parts of the gamma activity are not derived from asymmetrical beta waveform and seem to be locked to the phase of beta (Fig. S2C). Having said this, neither the sharpness nor the steepness index was significantly altered by DBS. In contrast, we did find significant beta (16–25 Hz) -high gamma (110–166 Hz) PAC reduction comparing DBS off *vs.* on. We propose that the following two, non-mutually exclusive possibilities could account for this discrepancy: first, a sizable part of our on *vs.* off beta-high gamma PAC is real, given the null effect of sharpness and steepness. Second, the sharpness index is not sensitive enough to capture the large number of combinations where high frequencies could yield a sharp waveform. We further note that at this stage, there is no methodological approach available to discern spurious coupling caused by non-sinusoidal wave morphology from actual cross-frequency coupling.

With respect to the source reconstruction used in the second part of the analysis, other nearby or contiguous active generators, such as the anterior cingulate cortex or dorsomedial prefrontal regions may possibly confound the localization of the observed effect to the ventromedial prefrontal cortex. Moreover, the signal may be potentially contaminated by ocular artifacts, especially considering that no simultaneous electrooculogram was recorded. However, by using ICA, we were able to identify and remove eye movement-related artifacts, which produce very clear patterns with stereotypical scalp distributions. Source reconstruction crucially improves the spatial resolution of the signals as well as the problem of infinite source configurations in sensor space [48,49].

Conclusion

Taken together, we provide evidence for abnormally increased coupling between the phase of beta (16–25 Hz) oscillations and amplitude of high gamma activity (110–166 Hz) in ventromedial frontal areas (fronto-central scalp sensors) in OCD patients, compared to healthy control subjects, akin to dysrhythmias observed in other neurological and psychiatric disorders. This pathological synchronization was normalized under DBS of the nucleus accumbens. Deciphering the mechanisms underlying the appearance of this aberrant oscillatory pattern could lead to better understanding of the pathophysiology of OCD as well as to novel therapeutic approaches, including non-invasive brain stimulation techniques targeting this dysrhythmia.

Funding

This work was supported by Project grants SAF2015-65982-R from the Spanish Ministry of Economy and Competitiveness to BS and PSI2014-58654-JIN to JGR, an FPI Predoctoral Fellowship (BES-

2016-079470) to ST, and BIAL Foundation Grant 119/12 to BS. This project has received funding from the European Research Council (ERC) under the European Union's Horizon 2020 research and innovation programme (ERC-2018-COG 819814).

CRediT authorship contribution statement

Svenja Treu: Writing – original draft, Visualization, Formal analysis, Investigation, Conceptualization. **Javier J. Gonzalez-Rosa:** Investigation, Resources, Writing – review & editing, Supervision. **Vanesa Soto-Leon:** Investigation, Resources. **Diego Lozano-Soldevilla:** Supervision, Formal analysis, Visualization, Writing – original draft, Conceptualization, Writing – review & editing. **Antonio Oliviero:** Project administration, Resources, Writing – review & editing. **Fernando Lopez-Sosa:** Investigation. **Blanca Reneses-Prieto:** Project administration, Resources. **Juan A. Barcia:** Project administration, Resources, Funding acquisition. **Bryan A. Strange:** Writing – review & editing, Funding acquisition, Project administration, Resources, Supervision, Conceptualization.

Declaration of competing interest

JAB has received travel and speaker honoraria from Medtronic and Boston Scientific. The rest of authors declare no conflicts of interest.

Appendix A. Supplementary data

Supplementary data to this article can be found online at https://doi.org/10.1016/j.brs.2021.04.028.

References

[1] American Psychiatric Association. American psychiatric association: Diagnostic and statistical Manual of Mental disorders. In: Text Revision. fourth ed. Am Psychiatr Assoc; 2000. https://doi.org/10.1176/appi.books.9780890423349.
[2] Ruscio AM, Stein DJ, Chiu WT, Kessler RC. The epidemiology of obsessive-compulsive disorder in the National comorbidity survey replication. Mol Psychiatr 2010:53–63. https://doi.org/10.1038/mp.2008.94.
[3] Harrison BJ, Soriano-Mas C, Pujol J, Ortiz H, López-Solà M, Hernández-Ribas R, et al. Altered corticostriatal functional connectivity in obsessive-compulsive disorder. Arch Gen Psychiatr 2009;66:1189–200. https://doi.org/10.1001/archgenpsychiatry.2009.152.
[4] Abe Y, Sakai Y, Nishida S, Nakamae T, Yamada K, Fukui K, et al. Hyper-influence of the orbitofrontal cortex over the ventral striatum in obsessive-compulsive disorder. Eur Neuropsychopharmacol 2015;25:1898–905. https://doi.org/10.1016/j.euroneuro.2015.08.017.
[5] Saxena S, Brody AL, Schwartz JM, Baxter LR. Neuroimaging and frontal-subcortical circuitry in obsessive-compulsive disorder. Br J Psychiatry 1998;173:26–37. https://doi.org/10.1192/s0007125000297870.
[6] Saxena S, Rauch SL. Functional neuroimaging and the neuroanatomy of obsessive-compulsive disorder. Psychiatr Clin 2000;23:563–86. https://doi.org/10.1016/S0193-953X(05)70181-7.
[7] Menzies L, Chamberlain SR, Laird AR, Thelen SM, Sahakian BJ, Bullmore ET. Integrating evidence from neuroimaging and neuropsychological studies of obsessive-compulsive disorder: the orbitofronto-striatal model revisited. Neurosci Biobehav Rev 2008;32:525–49. https://doi.org/10.1016/j.neubiorev.2007.09.005.
[8] Smith EE, Schüller T, Huys D, Baldermann JC, Andrade P, Allen JJ, et al. A brief demonstration of frontostriatal connectivity in OCD patients with intracranial electrodes. Neuroimage 2020;220:117138. https://doi.org/10.1016/j.neuroimage.2020.117138.
[9] Figee M, Luigjes J, Smolders R, Valencia-Alfonso C-E, Van Wingen G, De Kwaasteniet B, et al. Deep brain stimulation restores frontostriatal network activity in obsessive-compulsive disorder. Nat Neurosci 2013;16:386.
[10] Smolders R, Mazaheri A, Van Wingen G, Figee M, De Koning PP, Denys D. Deep brain stimulation targeted at the nucleus accumbens decreases the potential for pathologic network communication. Biol Psychiatr 2013;74:e27–8. https://doi.org/10.1016/j.biopsych.2013.03.012.
[11] Uhlhaas PJ, Singer W. Neural synchrony in brain disorders: relevance for cognitive dysfunctions and pathophysiology. Neuron 2006;52:155–68. https://doi.org/10.1016/j.neuron.2006.09.020.
[12] Buzsáki G, Watson BO. Brain rhythms and neural syntax: implications for efficient coding of cognitive content and neuropsychiatric disease. Dialogues Clin Neurosci 2012;14:345–67.
[13] De Hemptinne C, Swann NC, Ostrem JL, Ryapolova-Webb ES, San Luciano M, Galifianakis NB, et al. Therapeutic deep brain stimulation reduces cortical phase-amplitude coupling in Parkinson's disease. Nat Neurosci 2015;18:779–86. https://doi.org/10.1038/nn.3997.
[14] Kondylis ED, Randazzo MJ, Alhourani A, Lipski WJ, Wozny TA, Pandya Y, et al. Movement-related dynamics of cortical oscillations in Parkinson's disease and essential tremor. Brain 2016. https://doi.org/10.1093/brain/aww144.
[15] Bahramisharif A, Mazaheri A, Levar N, Richard Schuurman P, Figee M, Denys D. Deep brain stimulation diminishes cross-frequency coupling in obsessive-compulsive disorder. Biol Psychiatr 2016;80:e57–8. https://doi.org/10.1016/j.biopsych.2015.05.021.
[16] Widge AS, Zorowitz S, Link K, Miller EK, Deckersbach T, Eskandar EN, et al. Ventral capsule/ventral striatum deep brain stimulation does not consistently diminish occipital cross-frequency coupling. Biol Psychiatr 2016;80:e59–60. https://doi.org/10.1016/j.biopsych.2015.10.029.
[17] Horn A, Li N, Dembek TA, Kappel A, Boulay C, Ewert S, et al. Lead-DBS v2: towards a comprehensive pipeline for deep brain stimulation imaging. Neuroimage 2019;184:293–316. https://doi.org/10.1016/j.neuroimage.2018.08.068.
[18] Tadel F, Baillet S, Mosher JC, Pantazis D, Leahy RM. Brainstorm: a user-friendly application for MEG/EEG analysis. Comput Intell Neurosci 2011;2011. https://doi.org/10.1155/2011/879716.
[19] Cardoso JF, Souloumiac A. Blind beamforming for non-Gaussian signals. IEE Proc - Part F Radar & Signal Process 1993;140:362–70. https://doi.org/10.1049/ip-f-2.1993.0054.
[20] Canolty RT, Edwards E, Dalal SS, Soltani M, Nagarajan SS, Kirsch HE, et al. High gamma power is phase-locked to theta oscillations in human neocortex. Science 2006;313(80-):1626–8. https://doi.org/10.1126/science.1128115.
[21] Oostenveld R, Fries P, Maris E, Schoffelen JM. FieldTrip: open source software for advanced analysis of MEG, EEG, and invasive electrophysiological data. Comput Intell Neurosci 2011. https://doi.org/10.1155/2011/156869.
[22] Maris E, Oostenveld R. Nonparametric statistical testing of EEG- and MEG-data. J Neurosci Methods 2007;164:177–90. https://doi.org/10.1016/j.jneumeth.2007.03.024.
[23] Shattuck DW, Leahy RM. Brainsuite: an automated cortical surface identification tool. Med Image Anal 2002;6:129–42. https://doi.org/10.1016/S1361-8415(02)00054-3.
[24] Cole SR, Voytek B. Brain oscillations and the importance of waveform shape. Trends Cognit Sci 2017;21:137–49. https://doi.org/10.1016/j.tics.2016.12.008.
[25] Kramer MA, Tort ABL, Kopell NJ. Sharp edge artifacts and spurious coupling in EEG frequency comodulation measures. J Neurosci Methods 2008;170:352–7. https://doi.org/10.1016/j.jneumeth.2008.01.020.
[26] Cole SR, van der Meij R, Peterson EJ, de Hemptinne C, Starr PA, Voytek B. Nonsinusoidal beta oscillations reflect cortical pathophysiology in Parkinson's disease. J Neurosci 2017;37:4830–40. https://doi.org/10.1523/JNEUROSCI.2208-16.2017.
[27] Jackson N, Cole SR, Voytek B, Swann NC. Characteristics of waveform shape in Parkinson's disease detected with scalp electroencephalography. ENeuro 2019;6. https://doi.org/10.1523/ENEURO.0151-19.2019.
[28] Özkurt TE, Schnitzler A. A critical note on the definition of phase-amplitude cross-frequency coupling. J Neurosci Methods 2011;201:438–43. https://doi.org/10.1016/j.jneumeth.2011.08.014.
[29] Barcia JA, Avecillas-Chasín JM, Nombela C, Arza R, García-Albea J, Pineda-Pardo JA, et al. Personalized striatal targets for deep brain stimulation in obsessive-compulsive disorder. Brain Stimul 2019;12:724–34. https://doi.org/10.1016/j.brs.2018.12.226.
[30] Lozano-Soldevilla D. NEURO FORUM Sensory Processing Nonsinusoidal neuronal oscillations: bug or feature? J Neurophysiol 2018;119:1595–8. https://doi.org/10.1152/jn.00744.2017.-There.
[31] Li N, Baldermann JC, Kibleur A, Treu S, Akram H, Elias GJB, et al. A unified connectomic target for deep brain stimulation in obsessive-compulsive disorder. Nat Commun 2020;11:3364. https://doi.org/10.1038/s41467-020-16734-3.
[32] Nachev P, Lopez-Sosa F, Gonzalez-Rosa JJ, Galarza A, Avecillas J, Pineda-Pardo JA, et al. Dynamic risk control by human nucleus accumbens. Brain 2015;138:3496–502. https://doi.org/10.1093/brain/awv285.
[33] Cohen MX, Axmacher N, Lenartz D, Elger CE, Sturm V, Schlaepfer TE. Good vibrations: cross-frequency coupling in the human nucleus accumbens during reward processing. J Cognit Neurosci 2009;21:875–89. https://doi.org/10.1162/jocn.2009.21062.
[34] Yang AI, Vanegas N, Lungu C, Zaghloul KA. Beta-coupled high-frequency activity and beta-locked neuronal spiking in the subthalamic nucleus of Parkinson's disease. J Neurosci 2014;34:12816–27. https://doi.org/10.1523/JNEUROSCI.1895-14.2014.
[35] Shreve LA, Velisar A, Malekmohammadi M, Koop MM, Trager M, Quinn EJ, et al. Subthalamic oscillations and phase amplitude coupling are greater in the more affected hemisphere in Parkinson's disease. Clin Neurophysiol 2017;128:128–37. https://doi.org/10.1016/j.clinph.2016.10.095.
[36] Burguière E, Monteiro P, Mallet L, Feng G, Graybiel AM. Striatal circuits, habits, and implications for obsessive-compulsive disorder. Curr Opin Neurobiol 2015;30:59–65. https://doi.org/10.1016/j.conb.2014.08.008.

[37] Robbins TW, Vaghi MM, Banca P. Obsessive-compulsive disorder: puzzles and prospects. Neuron 2019;102:27–47. https://doi.org/10.1016/j.neuron.2019.01.046.
[38] Marco-Pallarés J, Münte TF, Rodríguez-Fornells A. The role of high-frequency oscillatory activity in reward processing and learning. Neurosci Biobehav Rev 2015;49:1–7. https://doi.org/10.1016/j.neubiorev.2014.11.014.
[39] Knutson B, Taylor J, Kaufman M, Peterson R, Glover G. Distributed neural representation of expected value. J Neurosci 2005;25:4806–12. https://doi.org/10.1523/JNEUROSCI.0642-05.2005.
[40] O'Doherty J, Rolls ET, Francis S, Bowtell R, McGlone F. Representation of pleasant and aversive taste in the human brain. J Neurophysiol 2001;85:1315–21. https://doi.org/10.1152/jn.2001.85.3.1315.
[41] Canolty RT, Knight RT. The functional role of cross-frequency coupling. Trends Cognit Sci 2010;14:506–15. https://doi.org/10.1016/j.tics.2010.09.001.
[42] De Hemptinne C, Ryapolova-Webb ES, Air EL, Garcia PA, Miller KJ, Ojemann JG, et al. Exaggerated phase-amplitude coupling in the primary motor cortex in Parkinson disease. Proc Natl Acad Sci U S A 2013;110:4780–5. https://doi.org/10.1073/pnas.1214546110.
[43] Miller KJ, Hermes D, Honey CJ, Hebb AO, Ramsey NF, Knight RT, et al. Human motor cortical activity is selectively phase-entrained on underlying rhythms. PLoS Comput Biol 2012;8. https://doi.org/10.1371/journal.pcbi.1002655.
[44] Yanagisawa T, Yamashita O, Hirata M, Kishima H, Saitoh Y, Goto T, et al. Regulation of motor representation by phase-amplitude coupling in the sensorimotor cortex. J Neurosci 2012;32:15467–75. https://doi.org/10.1523/JNEUROSCI.2929-12.2012.
[45] Heilbron K, Noyce AJ, Fontanillas P, Alipanahi B, Nalls MA, Cannon P. The Parkinson's phenome–traits associated with Parkinson's disease in a broadly phenotyped cohort. NPJ Parkinson's Dis. 2019;5(1):1–8.
[46] Grover S, Nguyen JA, Viswanathan V, Reinhart RMG. High-frequency neuromodulation improves obsessive-compulsive behavior. Nat Med 2021:1–7. https://doi.org/10.1038/s41591-020-01173-w.
[47] Gong R, Wegscheider M, Mühlberg C, Gast R, Fricke C, Rumpf J-J, et al. Spatiotemporal features of β-γ phase-amplitude coupling in Parkinson's disease derived from scalp EEG. Brain 2020. https://doi.org/10.1093/brain/awaa400.
[48] Yao J, Dewald JPA. Evaluation of different cortical source localization methods using simulated and experimental EEG data. Neuroimage 2005;25:369–82. https://doi.org/10.1016/j.neuroimage.2004.11.036.
[49] Koles ZJ. Trends in EEG source localization. Electroencephalogr Clin Neurophysiol 1998;106:127–37. https://doi.org/10.1016/S0013-4694(97)00115-6.